

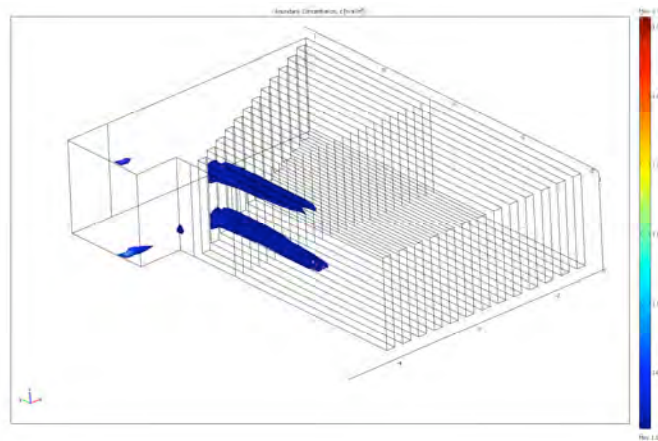
Evaluation of Concentration Variance as a Function of Z'/Pe in a Micro fluidic Device

Chem E 499

Mentor: Professor Emeritus Bruce Finlayson

Jordan Flynn

Friday, June 6, 2008



Introduction

The purpose of this research is to characterize the mixing in a micro fluidic device. This will be achieved by looking at the variance (a measure of mixing) versus the length of the device divided by the Peclet number (Z'/Pe). From looking at graphs of variance versus Z'/Pe we expect to see a relationship. To test this relationship, the length of the device will be varied from one half unit in length to two and a half units in length. The Peclet numbers will be chosen at different lengths so that the ratio of Z'/Pe will be identical for five points, one at each of the different lengths. Each of the five data sets will then be graphed and a relationship should be present between these ratios of Z'/Pe and the variance.

Another graph will be created with Peclet numbers ranging from 10 to 1,000 in different length devices to create a large range of values to see if a consistent trend is followed in a wider range of Z'/Pe values.

The 2-D geometry will be compared to a 3-D geometry to assess the differences in mixing that takes place in a 3-D mixer as compared to the 2-D version of the device. In addition, the variance data will be compared to the variance data for a T sensor to compare how efficient of a mixer my micro fluidic device is compared to a T sensor.

The Problem in Detail

To solve this problem, the Incompressible Navier-Stokes equation and the Convection and Diffusion equation will be solved simultaneously in their non-dimensional forms.

For the Navier-Stokes equation, we start out with the dimensional form of the equation:

$$\rho \frac{\partial u}{\partial t} + \rho u \cdot \nabla u = -\nabla p + \mu \nabla^2 u$$

To non-dimensionalize this equation we then define the following quantities:

$$u' = \frac{u}{u_s}, \quad p' = \frac{p}{p_s}, \quad x' = \frac{x}{x_s}, \quad \nabla = x_s \nabla$$

This equation can then be arranged to give the following non-dimensional form:

$$\frac{\partial u'}{\partial t} + Re u' \cdot \nabla' u' = -\nabla' p' + \nabla'^2 u'$$

In the non dimensional form of the Navier-Stokes equation, the dynamic viscosity (μ) is set equal to one and the density (ρ) is set equal to one. A normal inflow velocity of one is used at the inlet of the device. The outlets have been set to a pressure of zero with no viscous stress. All other boundaries of the device are walls with a no slip boundary condition.

For the Convection and Diffusion Equation we will solve the equation in a non dimensional form. The Convection and Diffusion equation we start with is:

$$\frac{\partial c}{\partial t} + v \cdot \nabla c = D \nabla^2 c$$

To make the equation dimensionless we define the following quantities:

$$c' = \frac{c}{c_s}, \quad v' = \frac{v}{v_s}, \quad \nabla' = x_s \nabla, \quad t' = \frac{tv_s}{x_s}$$

The Convection and Diffusion equation then becomes:

$$\frac{\partial c'}{\partial t'} + v' \cdot \nabla' c' = \frac{1}{Pe} \nabla'^2 c'$$

Since the non-dimensional form of the equation will be used, $D = \frac{1}{Pe}$ and we can

simply put in — for diffusivity to vary our Peclet number in the sub domain settings.

Also in the sub domain settings the x and y velocities are set to u and v respectively which are quantities solved for in the Navier-Stokes Equations. The upper half of the inlet is set to a concentration of zero and the lower half is set to a concentration of one in the boundary conditions. The outlets are set to convective flux and all other walls are set to insulation/symmetry.

A picture of the device follows with the dimensions of the device:

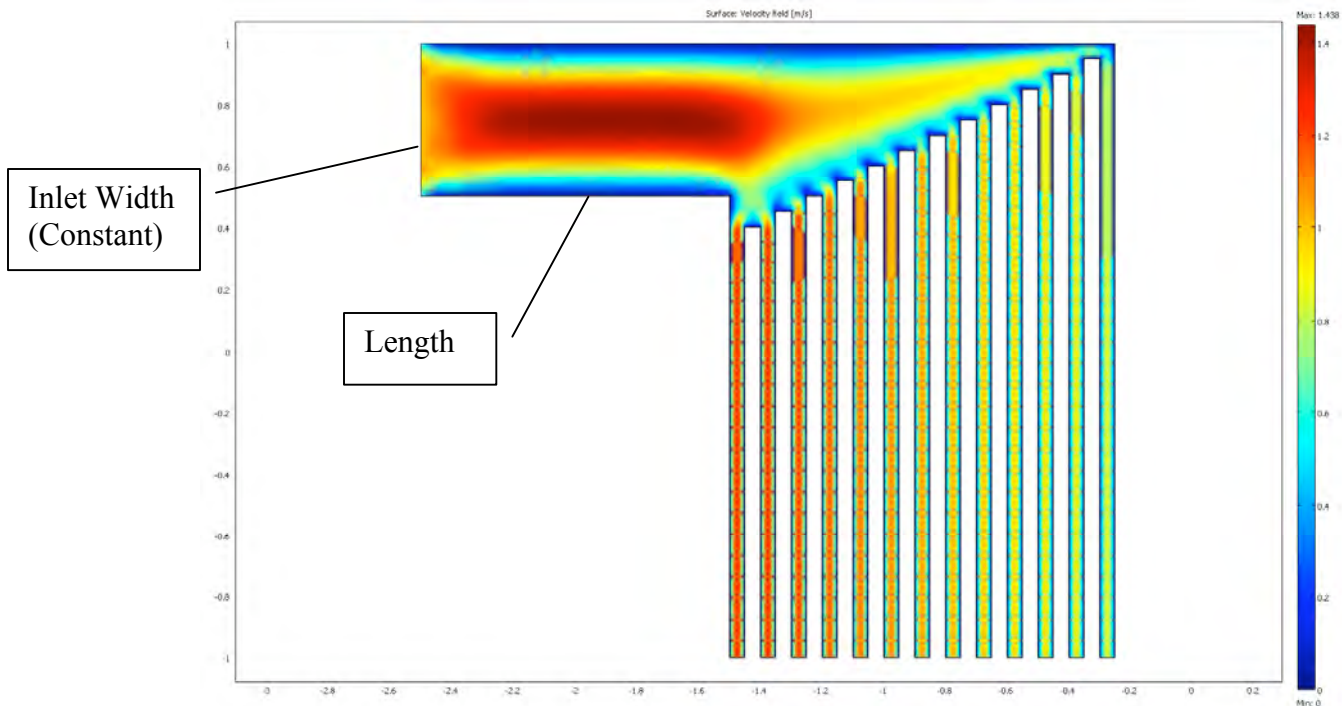


Figure 1. The dimensions on this device are one unit for the inlet width, and .1 units for the width of each outlet. The length in the above device was varied from 0.5 units to 2.5 units while all other dimensions were kept constant. This figure shows the velocity field present in a device with a Peclet number of 200 and a length of one unit.

To calculate the variance in the device, the mixing cup concentration must be determined using the following equation:

$$C_{mixingcup} = \frac{\int_A c(x, y, z) v(x, y) dx dy}{\int_A v(x, y) dx dy} = .5$$

In the mixing cup concentration equation, c is concentration and v is the velocity. This equation is integrated over A , the area of the boundary. Since half the inlet is at a concentration of zero and half at a concentration of one the $c_{mixingcup}$ will be equal to 0.5.

From this the variance can be calculated using the following equation:

$$C_{variance} = \frac{\sum_{i=1}^n \int_A [c_i(x, y, z) - c_{mixingcup}]^2 v_i(x, y) dA_i}{\sum_{i=1}^n \int_A v_i(x, y) dA_i}$$

Boundary integrations are performed across all outlet boundaries and the inlet boundary to give the desired quantities.

Results

Figure two shows a plot of Z'/Pe versus the variance for the five cases with the same Z'/Pe ratios in five different length devices:

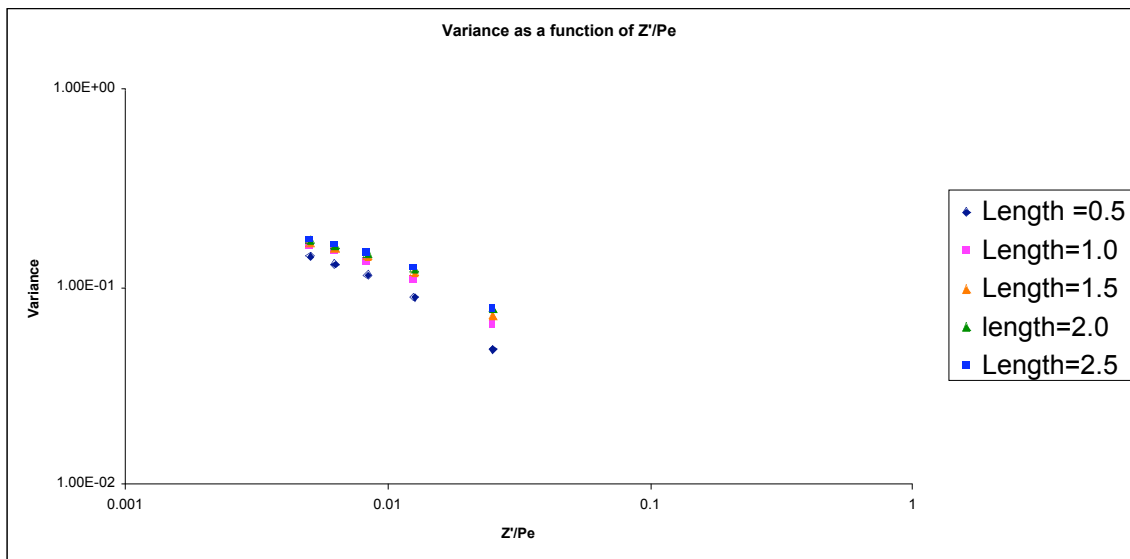


Figure 2. This Figure shows a plot of the variance versus the length over Peclet number. Notice that the relationship is consistent for all devices despite different dimensions of the device.

The results of the calculations presented in the graph above have been verified by hand for the case with a length of 2.5 and a Peclet number of 100 (See Appendix). Identical calculations were used to obtain the results for the other cases. The typical mesh solved for has approximately 1,600 elements and around 13,000 degrees of freedom.

The effects of mesh refinement were determined by refining the mesh of a particular case and examining its effects on the calculated variance.

Effects of a More Refined Mesh

L=1 Pe=2.5

	Case 1	Case 2	Case 3
Elements	1612	6448	16302
Degrees of Freedom	12946	46844	113898
Solution Time (s)	4.204	17.062	43.297
Variance	9.55E-02	9.89E-02	9.95E-02
Percent Error From Best Solution	3.96	0.55	0

Figure 3. This table compares the results of calculating the variance with a more refined mesh. The Percent error is determined by $\%Error = \frac{(\text{var}_1 - \text{var}_2)}{\text{var}_2} \cdot 100$. The Best possible solution was obtained by continuing to refine the mesh and solve the problem until the computer ran out of memory to solve the problem.

This table shows that the error in using an unrefined mesh has a less than 5% error from the best solution obtainable.

The results for a larger range of Z'/Pe data have been tabulated and presented below in Figure 4.

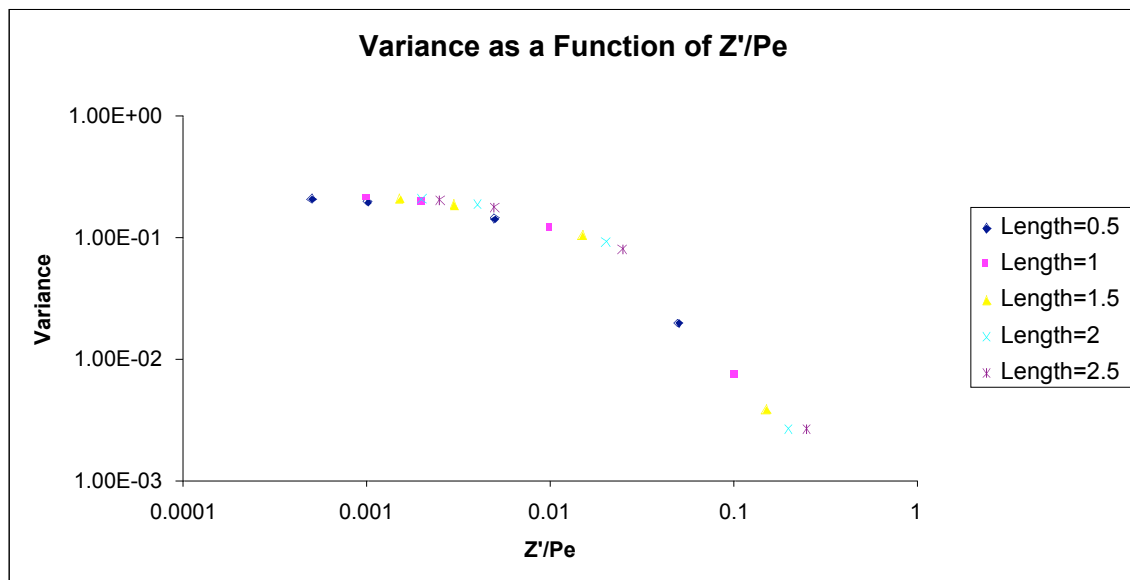


Figure 4. This figure presents data of Z'/Pe in a wider range. The Peclet numbers in this data were ranged from 10 to 1,000.

The data presented in figure four show that the variance follows a distinct curve regardless of the dimensions or Peclet number of the device. The only quantity that matters is Z'/Pe which characterizes the mixing of the device.

To examine the effects of a 3-D geometry versus a 2-D geometry, the calculations presented in the graph of figure five were carried out.

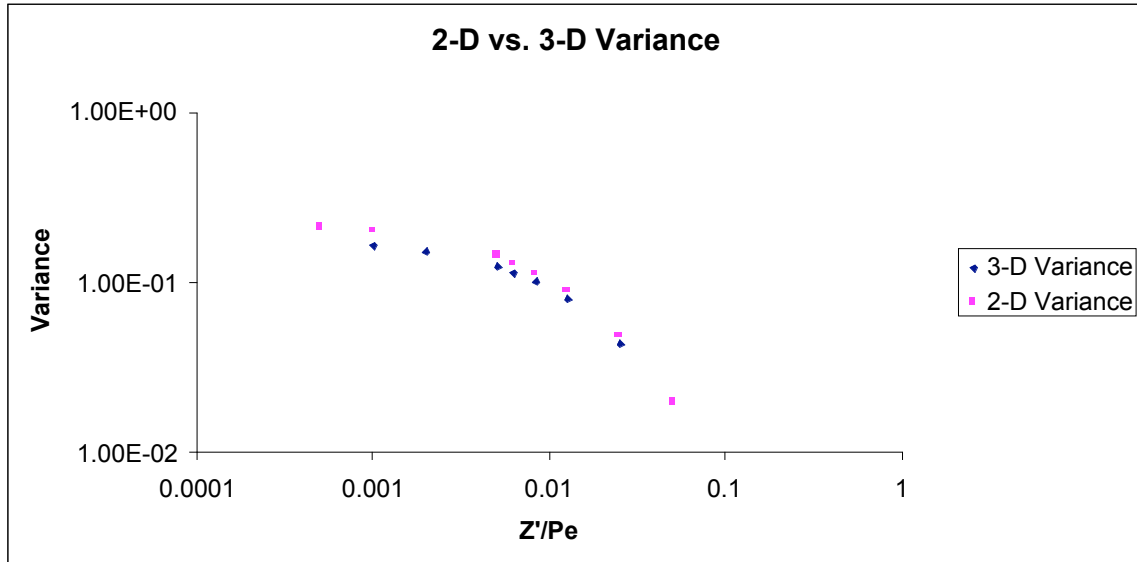


Figure 5. This figure compares the variance of a 2-D model against a 3-D model. The calculations were carried out at a range of Peclet numbers with a length of 0.5 units. The 3-D geometry has been extruded by one unit.

From the results of figure five, a conclusion can be drawn that there is not a significant difference between the 3-D and 2-D models. The small change in variance of a 3-D model can be attributed to the no slip conditions applied to four surfaces instead of two, which slows down the flow and allows slightly more diffusion than the 2-D geometry.

To compare the mixing obtained in my micro fluidic device to that of a T sensor, a plot of variance comparing both devices has been constructed.

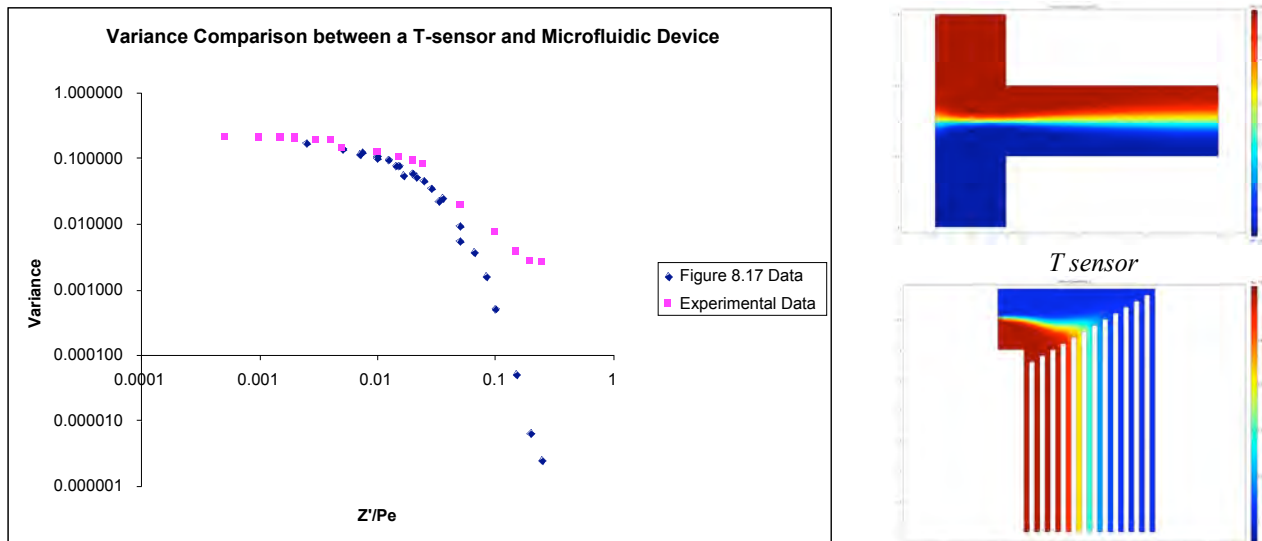


Figure 6. This figure compares the variance of a T sensor to the research geometry. The actual geometries are shown at the right of the variance graph.

In figure six, it is seen that the variance of a T sensor is lower and therefore the T sensor is a better mixer than the geometry chosen for research.

Comparisons to Literature Data

For the results obtained above it is important that they compare to the paper “Generating fixed concentration arrays in a micro fluidic device,” by Holden ET. All Comparisons can be drawn between the authors of this paper and my own simulations to verify the simulations that I have performed are correct. I have verified the papers results by plotting the wall concentration and examining the effects of an increasing flow rate on concentration plots.

The wall concentration from the literature results and my own simulation are presented in figure seven.

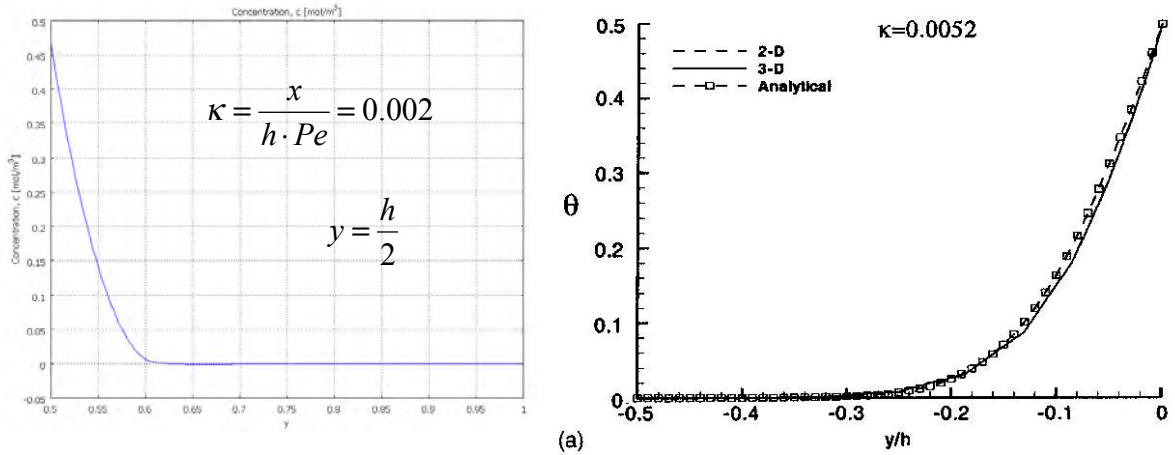


Figure 7. The wall concentrations plotted across half of the inlet channel at the start of the first micro channel outlet. The definition of θ is given in the experimental data (left) which is compared to the literature data. $X=0.5$ and $Pe=250$ for the experimental data.

The diffusion of the dye in the literature data has diffused out from the wall farther than in the experimental data. This result is consistent because of the values of θ . As the Peclet number increases the θ value decreases allowing less diffusion to take place. Since the experimental results plot a lower concentration across the half channel, these results are consistent.

Another check between the literature and experimental data is the comparison of concentration plots. The literature plots concentration as the flow rate of the device is increased from 50 to 500 nL/min. To simulate this change in flow rate I have created plots of concentration across the channels with varying Peclet numbers. The results show that the literature and the experimental data agree qualitatively. As the Peclet number and flow rate increases, the mixing that takes place in the device decreases. This decrease in mixing is evident by the amount of outlets with concentrations around zero and one. Near the edges of the device, as the flow rate increases, less time is available for diffusion to occur in the device, creating a steeper variation of concentrations that is present in both literature and experimental data. These results are presented in the Appendix.

Conclusions:

As can be seen from the graphs above, as Z'/Pe increases, the variance becomes smaller. This trend is consistent for various lengths and could be extended to approximate the relationship for other devices of this type. The effect on variance by using a 2-D versus 3-D model for this micro fluidic device is very small and well within an order of magnitude. Since the 2-D and 3-D results are comparable, a 2-D geometry may be used to approximate results that would be obtained in 3-D modeling of similar devices. Finally, the micro fluidic device chosen is a less successful mixer than a T sensor.

Appendix:

Results Tables:

Table of Results (Width=.5) Used in Sample Calculation				
z (Dimensionless)	Peclet Number (Dimensionless)	z'/Pe (Dimensionless)	Variance (Dimensionless)	
0.5	20	0.025	0.00777	
0.5	40	0.0125	0.02711	
0.5	60	0.00833	0.04895	
0.5	80	0.00625	0.06786	
0.5	100	0.005	0.08335	
1	40	0.025	0.00831	
1	80	0.0125	0.03314	
1	120	0.00833	0.05747	
1	160	0.00625	0.07663	
1	200	0.005	0.09138	
1.5	60	0.025	0.02010	
1.5	120	0.0125	0.04532	
1.5	180	0.00833	0.07019	
1.5	240	0.00625	0.08963	
1.5	300	0.005	0.10447	
2	80	0.025	0.02046	
2	160	0.0125	0.04732	
2	240	0.00833	0.07266	
2	320	0.00625	0.09193	
2	400	0.005	0.10638	
2.5	100	0.025	0.01974	
2.5	200	0.0125	0.04501	
2.5	300	0.00833	0.06844	
2.5	400	0.00625	0.08678	
2.5	500	0.005	0.10121	

2-D Data at Chosen Ratios (Width =1) Figure 4

Z' (Dimensionless)	Pe (Dimensionless)	Z'/Pe (Dimensionless)	Variance (Dimensionless)	Pressure Drop (Dimensionless)
0.5	20	0.0250	4.84E-02	2974
0.5	40	0.0125	8.93E-02	2974
0.5	60	0.0083	1.14E-01	2974
0.5	80	0.0063	1.31E-01	2974
0.5	100	0.0050	1.43E-01	2974
1	40	0.0250	6.42E-02	2981
1	80	0.0125	1.10E-01	2981
1	120	0.0083	1.34E-01	2981
1	160	0.0063	1.50E-01	2981
1	200	0.0050	1.61E-01	2981
1.5	60	0.0250	7.25E-02	2986
1.5	120	0.0125	1.19E-01	2986
1.5	180	0.0083	1.43E-01	2986
1.5	240	0.0063	1.58E-01	2986
1.5	300	0.0050	1.68E-01	2986
2	80	0.0250	7.76E-02	2991
2	160	0.0125	1.24E-01	2991
2	240	0.0083	1.48E-01	2991
2	320	0.0063	1.63E-01	2991
2	400	0.0050	1.74E-01	2991
2.5	100	0.0250	8.12E-02	3007
2.5	200	0.0125	1.27E-01	3007
2.5	300	0.0083	1.50E-01	3007
2.5	400	0.0063	1.63E-01	3007
2.5	500	0.0050	1.72E-01	3007

2-D Data at a Large Range (Width=1) Figure 4, Figure 6

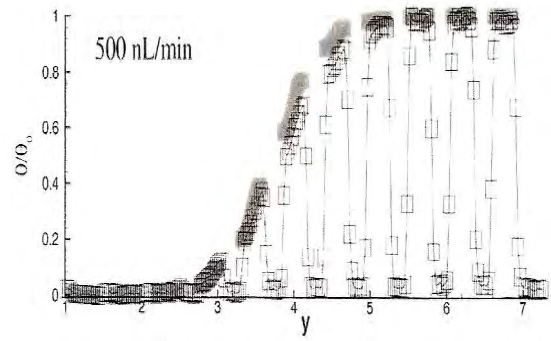
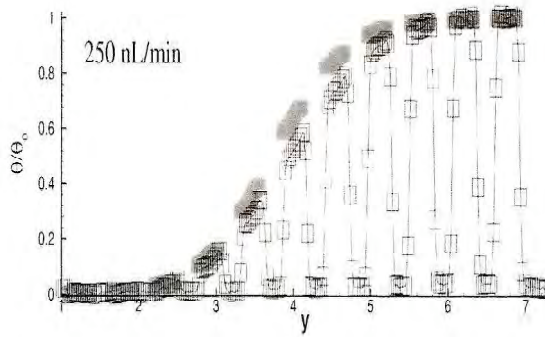
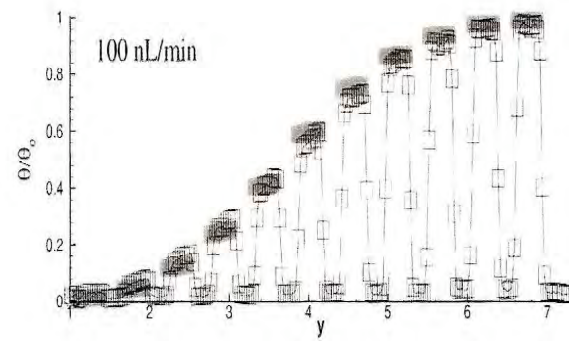
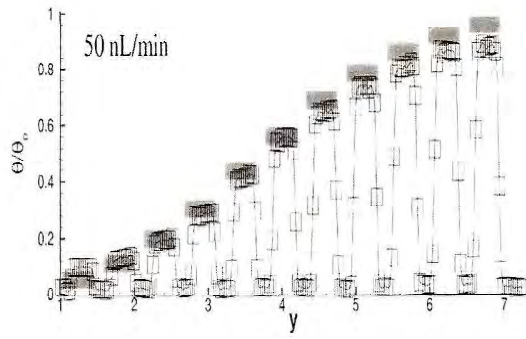
Z' (Dimensionless)	Pe (Dimensionless)	Z'/Pe (Dimensionless)	Variance (Dimensionless)	Pressure Drop (Dimensionless)
0.5	10	0.05	0.0199	2974
0.5	100	0.005	0.1456	2974
0.5	500	0.001	0.2000	2974
0.5	1000	0.0005	0.2112	2974
1	10	0.1	0.0075	2980
1	100	0.01	0.1234	2980
1	500	0.002	0.1974	2980
1	1000	0.001	0.2148	2980
1.5	10	0.15	0.0039	2986
1.5	100	0.015	0.1067	2986
1.5	500	0.003	0.1874	2986

1.5	1000	0.0015	0.2084	2986
2	10	0.2	0.0027	2993
2	100	0.02	0.0935	2993
2	500	0.004	0.1868	2993
2	1000	0.002	0.2126	2993
2.5	10	0.25	0.0026	3000
2.5	100	0.025	0.0819	3000
2.5	500	0.005	0.1787	3000
2.5	1000	0.0025	0.2038	3000

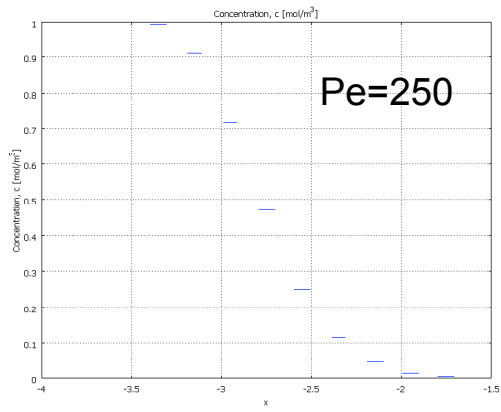
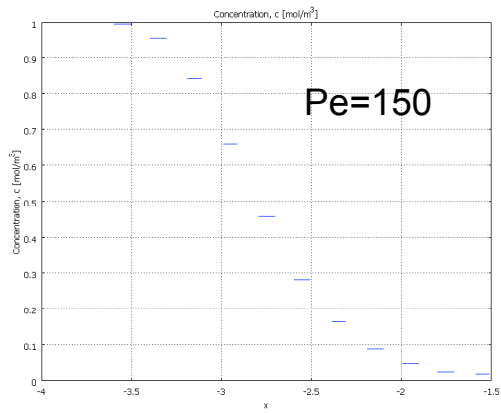
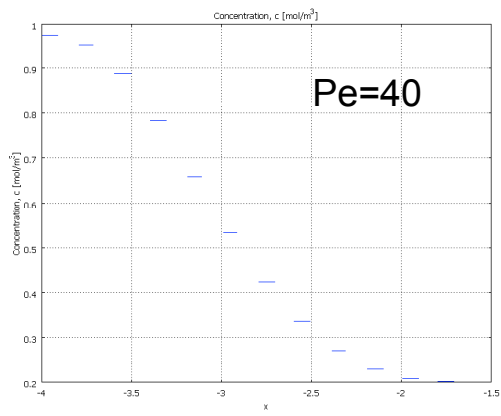
T Sensor Data Figure 6

Z'/Pe	Variance
0.0000	0.1876
0.0050	0.1359
0.0100	0.1026
0.0150	0.0780
0.0200	0.0593
0.0250	0.0453
0.0000	0.1745
0.0071	0.1144
0.0143	0.0772
0.0214	0.0523
0.0286	0.0355
0.0357	0.0242
0.0000	0.1347
0.0167	0.0543
0.0333	0.0222
0.0500	0.0091
0.0667	0.0037
0.0833	0.0016
0.0000	0.0581
0.0500	0.0054
0.1000	0.0005
0.1500	0.0001
0.2000	0.0000
0.2500	0.0000
0.0000	0.2048
0.0025	0.1689
0.0050	0.1443
0.0075	0.1248
0.0100	0.1085
0.0125	0.0946

Literature Concentration Plots



Experimental Concentration Plots



Sample Calculation of Variance:

Calculation of the Variance of Figure 1 geometry with Width=0.5, L=2.5 and Pe=100

Start with the Equation for Variance:

$$C_{\text{variance}} = \frac{\sum_{i=1}^n \int_A \left[c_i(x, y, z) - c_{\text{mixingcup}} \right]^2 v_i(x, y) dA_i}{\sum_{i=1}^n \int_A v_i(x, y) dA_i}$$

We will evaluate the top half of the integral by doing boundary integrations on each outlet with the $c_{\text{mixingcup}}$ equal to .5.

$$\text{Integration 1: } \int_{A_1} \left[c_1(x, y) - c_{\text{mixingcup}} \right]^2 v_1(x, y) dA_1 = .002421$$

$$\text{Integration 2: } 0.002163$$

$$\text{Integration 3: } 0.001626$$

$$\text{Integration 4: } 0.001126$$

$$\text{Integration 5: } 7.258641e-4$$

$$\text{Integration 6: } 4.39248e-4$$

$$\text{Integration 7: } 2.459387e-4$$

$$\text{Integration 8: } 1.32477e-4$$

$$\text{Integration 9: } 6.957116e-5$$

$$\text{Integration 10: } 3.768569e-5$$

$$\text{Integration 11: } 2.435543e-5$$

$$\text{Integration 12: } 1.98145e-5$$

$$\text{Integration 13: } 1.827043e-5$$

Next the total is computed by summing all of the 13 channels:

$$\sum_{i=1}^{13} \int_A \left[c_i(x, y, z) - c_{\text{mixingcup}} \right]^2 v_i(x, y) dA_i = 9.049225e-3$$

To compute the bottom of the integral we use continuity to note that:

$$\sum_{i=1}^{13} \int_A v_i(x, y) dA_i = \int v_{in} dA_{in} = .45833$$

Variance is therefore:

$$\frac{\sum_{i=1}^{13} \int_A \left[c_i(x, y, z) - c_{\text{mixingcup}} \right]^2 v_i(x, y) dA_i}{\int v_{in} dA_{in}} = 1.974e-2$$
 This hand calculation agrees with the

entry in the table above for variance with a width of 0.5, Pe=100 and a length=2.5.